

VELOCITY MEASUREMENT USING ANGULAR- AND FREQUENCY-CORRELATION TECHNIQUES

John A. Catton
Yasuo Kuga
Akira Ishimaru

University of Washington
Seattle, WA USA

I. Introduction

Detecting and estimating the velocity of slowly moving targets from a moving platform is difficult due to the Doppler broadening of the ground clutter. The latest MTI (moving target indicator) technique employs STAP (space-time adaptive processing) to reduce the clutter's signal and thus, is able to detect the target's speed [1]. This technique has proven to be very effective for detecting high-speed targets and also for some slower moving targets such as helicopters. If, however, the target's speed is small, such as ground targets, the target's signal is reduced along with the clutter, again rendering the detection of target's speed difficult.

The techniques described in this paper utilize the signals from a multiple sensor system and are based on the correlation of the scattered waves of the target [2-4]. The Doppler shift of the correlation function is then used to obtain the target's velocity. Unlike conventional MTI radar, our technique makes use of the Doppler shifted phase of the correlation of the scattered waves. Controlled experiments were conducted with an X-band radar and good agreement was obtained with numerical simulations.

II. Theory: Angular-Correlation Technique (ACT)

We assume that the airborne SAR is flying in the x -direction [4]. The platform has two radar sensors mounted along the x -direction (along-track) and two other sensors mounted along the y -direction (across-track). In the simplest configuration, the proposed correlation function can be obtained with only one transmitting antenna and two or more receiving antennas. To simplify the problem, we assume that both the target vehicle and SAR are on the same x - y plane and there is no z dependence. One pair of T_r (transmitter) and R_c (receiver) is located at x_n and x_{n+d} , and operating at ω . Similarly, another pair T_r' and R_c' is located at x_n' and $x_{n'+d}$, and operating at ω' as shown in Figure 1.

We consider the generalized correlation function of two sensors, which includes frequency and angles. The angles are related to the location of the target with respect to the radar sensors. Let E_r be the received signal at R_c due to T_r as shown in Figure 1.

$$E_r = \frac{e^{ikR}}{R} f(\hat{\theta}, \hat{i}, \omega) e^{ik(\hat{i}-\hat{\theta})\bar{r}-i\omega t} \quad (1)$$

where $f(\hat{\theta}, \hat{i}, \omega)$ is a scattering amplitude of the target, R is a distance between a target and sensor, and k is a wave-number.

Similarly, E_r' is the received signal at R_c' due to T_r'

$$E_r' = \frac{e^{ikR'}}{R'} f(\hat{\theta}', \hat{i}', \omega') e^{ik(\hat{i}'-\hat{\theta}')\bar{r}'-i\omega' t'} \quad (2)$$

The correlation of two received signals is given by [5]

$$\begin{aligned} \Gamma &= \langle E_r(t) E_r'^*(t') \rangle \\ &= \frac{e^{ikR-ik'R'}}{RR'} \iint e^{ik(\hat{i}-\hat{\theta})\bar{r}-i\omega t} e^{-ik(\hat{i}'-\hat{\theta}')\bar{r}'+i\omega' t'} \end{aligned} \quad (3)$$

where,

$$\begin{aligned} \bar{k}_s &= k(\hat{i}-\hat{\theta}), \quad \bar{k}_s' = k'(\hat{i}'-\hat{\theta}') \\ \bar{r}_c &= \frac{\bar{r} + \bar{r}'}{2}, \quad \bar{r}_d = \bar{r} = \bar{r}' = \bar{V}t_d \\ \omega_c &= \frac{\omega + \omega'}{2}, \quad \omega_d = \omega - \omega' \\ t_c &= \frac{t + t'}{2}, \quad t_d = t - t' \\ \bar{V} &= \bar{V}_x + \bar{V}_y \end{aligned} \quad (4)$$

To obtain the Doppler shift, we take the Fourier transform of Eq. (3) and get

$$\begin{aligned}
W(\omega) &= \int \langle E_R E_R^* \rangle e^{i\omega t_d} dt_d \\
&= \frac{e^{i(kR - k'R')}}{RR'} f(\omega) f^*(\omega') \\
&\quad e^{i(\bar{k}_s - \bar{k}'_s) \cdot \bar{r}_c - i\omega_d t_c}
\end{aligned} \tag{5}$$

$$\begin{aligned}
&\int e^{-i\omega_c t_d} e^{i\left(\frac{\bar{k}_s + \bar{k}'_s}{2}\right) \cdot \bar{V} t_d} e^{i\omega t_d} dt_d \\
&\int e^{-i\omega_c t_d} e^{i\left(\frac{\bar{k}_s + \bar{k}'_s}{2}\right) \cdot \bar{V} t_d} e^{i\omega t_d} dt_d = \\
&\quad \delta\left(\omega - \omega_c + \left(\frac{\bar{k}_s + \bar{k}'_s}{2}\right) \cdot \bar{V}\right)
\end{aligned} \tag{6}$$

If the target is not moving ($V = 0$), the delta function gives a non-zero value at $\omega = \omega_c$. However, if $V \neq 0$, the Doppler shifted frequency ω_{dop1} is given by

$$\begin{aligned}
\omega &= \omega_c - \left(\frac{\bar{k}_s + \bar{k}'_s}{2}\right) \cdot \bar{V} \\
&= \omega_c + \omega_{dop1}
\end{aligned} \tag{7}$$

$$\omega_{dop1} = -\left[\frac{k(\hat{i} - \hat{o}) + k'(\hat{i}' - \hat{o}')}{2}\right] \cdot \bar{V} \tag{8}$$

Equation (7) shows that the Doppler shift is related to both the sensor locations with respect to the target (angles) and operating frequencies. Furthermore, the expression for ω_{dop1} in Eq. (8) is given by the average of the Doppler frequencies measured by the two individual sensors.

III. Simulations (ACT)

For the simulation, a system resembling a ground-based system measuring the 2-dimensional velocity of a land vehicle is assumed. Figure 2 shows the configuration of the four sensors and the single transmitter. In this configuration, two Doppler frequencies are computed corresponding to the angular-correlation of the along-track (x -direction) and the across-track (y -direction) sensors. The effect of ground clutter is not incorporated into the simulation at this time.

In principle, the velocity vector may be obtained by a simple matrix inversion of Eq. (8). It was observed, however, that the inversion became unstable when the height of the platform (h_z) was close to zero. As the height of the platform increased, the inversion became more unstable, with the worst case directly over the target vehicle.

In order to improve stability, multiple platform locations were used to form a least-squares solution. Using both the along-track and across-track Doppler shifts, the expected Doppler shift predicted by Eq. (6) at the n^{th} platform location is given as

$$\begin{aligned}
\begin{bmatrix} \omega_{dop1p} \\ \omega_{dop1s} \end{bmatrix}_n &= \begin{bmatrix} c_{11} & c_{12} \\ c_{21} & c_{22} \end{bmatrix}_n \begin{bmatrix} V_x \\ V_y \end{bmatrix} \\
\bar{\omega}_n &= \mathbf{C}_n \bar{V}
\end{aligned} \tag{9}$$

where ω_{dop1p} is the Doppler shift in the along-track direction and ω_{dop1s} is the Doppler shift in the across-track direction. Taking N platform locations and starting at the n^{th} position, the resulting least-squares problem is defined by

$$\begin{aligned}
\begin{bmatrix} \bar{\omega}_n \\ \vdots \\ \bar{\omega}_{n+N-1} \end{bmatrix} &= \begin{bmatrix} \mathbf{C}_n \\ \vdots \\ \mathbf{C}_{n+N-1} \end{bmatrix} \bar{V} \\
\bar{\omega}_n^N &= \mathbf{C}_n^N \bar{V}
\end{aligned} \tag{10}$$

with the solution,

$$\bar{V}_{estimate} = \left(\mathbf{C}_n^{N^T} \mathbf{C}_n^N\right)^{-1} \mathbf{C}_n^{N^T} \bar{\omega}_n^N \tag{11}$$

Figure 3 shows the results of the least-squares solution using a constant viewing angle where N is dynamically chosen such that the angle between the "target-to- n^{th} platform location" and "target-to- $(n+N-1)^{\text{th}}$ platform location" vectors is constant. In this case, the viewing angle was set to $\sim 8.3^\circ$ at a platform height (h_z) equal to zero and down-range (h) of 1000m. The noise is white Gaussian with standard deviation $\sigma = 0.05$.

IV. Modified Theory: Angular-Velocity Technique (AVT)

While the ACT described in section II is expected to have good clutter rejection [6], the inversion may become unstable if the signal-to-noise ratio is poor. In order to improve the inversion stability further, the ACT must be modified. Assuming the configuration used in section II, the signals from the two receivers are given by E_r and E'_r defined in Eq. (1) and (2), respectively. Let the function F be defined as the conjugate multiplication of the two signals, observed different frequencies and angles but at the same time.

$$\begin{aligned}
F &= E_r(t)E_r'^*(t) \\
&= \frac{e^{i(kR-k'R')}}{RR'} f(\hat{i}, \hat{\delta}, \omega) f(\hat{i}', \hat{\delta}', \omega') e^{i(\bar{k}_s - \bar{k}_s')\bar{r} - \omega_d t} \quad (12)
\end{aligned}$$

where \bar{k}_s, \bar{k}_s' , and ω_d are defined by the relations of Eq. (4) and the identity $\bar{r}(t) = \bar{r}'(t)$ is used.

To determine the Doppler shift, we calculate the temporal frequency spectrum (W) of F

$$\begin{aligned}
\Gamma' &= F(t)F'^*(t') \\
&= \frac{|f(\hat{i}, \hat{\delta}, \omega) f(\hat{i}', \hat{\delta}', \omega')|^2}{R^2 R'^2} e^{i(\bar{k}_s - \bar{k}_s')\bar{r}_d - \omega_d t_d} \quad (13)
\end{aligned}$$

$$\begin{aligned}
W'(\omega) &= \int \Gamma' e^{i\omega t_d} dt_d \\
&= \frac{|f(\hat{i}, \hat{\delta}, \omega) f(\hat{i}', \hat{\delta}', \omega')|^2}{R^2 R'^2} \int e^{i(\bar{k}_s - \bar{k}_s')\bar{v}_d t_d + i(\omega - \omega_d)t_d} dt_d \\
&= \int e^{i(\bar{k}_s - \bar{k}_s')\bar{v}_d t_d + i(\omega - \omega_d)t_d} dt_d = \\
&\quad \delta(\omega - \omega_d + (\bar{k}_s - \bar{k}_s') \cdot \bar{V}) \quad (14)
\end{aligned}$$

For a stationary target ($V = 0$), the delta function of Eq. (14) yields a non-zero value at $\omega = \omega_d$. However, if the target is moving, the Doppler shifted frequency ω_{dop2} is given by

$$\begin{aligned}
\omega &= \omega_d - (\bar{k}_s - \bar{k}_s') \cdot \bar{V} \\
&= \omega_d + \omega_{dop2} \\
\omega_{dop2} &= -(\bar{k}_s - \bar{k}_s') \cdot \bar{V} \quad (15)
\end{aligned}$$

Similar to what was found for the ACT, the AVT results of Eq. (14) show the total Doppler shift is related to both the relative locations of the sensors to the target as well as the operating frequencies. The dependence of the Doppler shift on the target's velocity however, has changed. This velocity dependence is given by ω_{dop2} in Eq. (15) and is equal to the difference of the Doppler frequencies measured by the two individual sensors as opposed by their average for ω_{dop1} .

V. Modified Simulation (AVT)

In order to compare simulation results for the AVT with the ACT, the configuration of the simulation system

was kept the same, resembling a ground-based system measuring the velocity of a ground vehicle. The configuration of the system is shown in Figure 2 with $h_z = 0$ for the ground-based system.

The results for such a system using the AVT still shows instability for h_z close to zero. However, as the height above the target vehicle increases, the inversion stability is also observed to increase, as demonstrated by Figure 4, where the height (h_z) is equal to the distance down-range (h). The results of Figure 4 are for the case when the distance from the transmitter to the target is 1000m at the platform location of $x = 0$ and both the across-track and along-track receiver/transmitter separations (l and d) are 10m. The noise is white Gaussian with a standard deviation of $\sigma = 0.05$.

VI. Experimental Setup and Results

In the experimental system, a total of four X-band receiving antennas (2 across-track, 2 along-track) surround a single transmitter as shown in Figure 5. The target is positioned at discrete locations by means of a translational stage, driven by a stepping motor. The target scattering data is obtained through an HP 8719D microwave network analyzer. The data acquisition is completely controlled through a computer as shown in Figure 6, controlling and obtaining data from the network analyzer in coordination with movement of the target and antenna selection. The use of a network analyzer should not be misinterpreted as the necessity of measuring absolute phase. Rather, accurate relative phase measurements are required for accurate Doppler measurements. This can be shown from either of the two formulations of sections II and IV.

In this experiment, since time is ambiguous, it is the target's displacement that is estimated rather than its velocity. The processing of the data implements the AVT discussed in section IV. Using two consecutive target locations ($x[n]$ and $x[n+1]$), the phase difference of the temporal correlation function given by Eq. (13) is obtained for both the along-track and the across-track sensors. From this data, the target's displacements in both the x - and y -directions are estimated by the matrix inversion described by Eq. (15).

The experiment considers the case of one platform location ($x = 0$), analogous to being directly over a ground target vehicle ($h_z = 0, h \neq 0$ in Figure 2). The results of the experiment are shown in Figure 7 with the distance from the transmitter to the target being 2m and a displacement of 1mm on the translational stage tilted at a 12° angle with respect to the horizontal. With this configuration, the target's displacement in the x -direction is 0.97815mm, and -0.20791mm in the y -direction. A total of 45 target positions were used, resulting in 44 estimates for the displacement. The average estimate for the displacement is

0.95479mm in the x -direction and -0.22357mm in the y -direction, an error of -2.4% and 7.5% respectively.

VII. Conclusions

Simulation and experimental results have been presented demonstrating the effectiveness of the angular-correlation technique. The simulation of the ACT shows that the velocity vector may be obtained through simple inversion when the SNR is large. In order to improve performance of this technique, additional inversion techniques need to be explored. Furthermore, improved inversion stability has been demonstrated to be inherent in the AVT described in section V.

The experimental results verify the validity of the AVT. Further development and testing of the system however, is still required. Some of these include the testing of the system at multiple platform locations. Additionally, simulation and experimental testing of the performance of both methods in the presence of ground clutter are needed.

VIII. References

- [1] M. Skilnik, *Radar Handbook*, McGraw Hill, New York, 1990
- [2] T. K. Chan, Y. Kuga, and A. Ishimaru, "Circular SAR Imaging Using Frequency and Angular Correlation Techniques in a Clutter Environment," *IEEE Trans. Geoscience and Remote Sensing*, 37:5, Sept. 1999.
- [3] A. Ishimaru, T.-K. Chan, and Y. Kuga, "An Imaging Technique Using Confocal Circular Synthetic Aperture Radar," *IEEE Trans. Geoscience and Remote Sensing*, Vol. 36, 5, 1524-1530, September, 1998
- [4] Y. Kuga, A. Ishimaru, J. A. Catton, and C. T. C. Le, "Detection of slowly moving targets using angular- and frequency-correlation techniques," *Microwave and Optical Technology Letters*, 1999.
- [5] A. Ishimaru, *Wave Propagation and Scattering in Random Media*, IEEE Press, Piscataway, New Jersey and Oxford University Press, Oxford, England, An IEEE-OUP Classic Redissue, 1997
- [6] T.-K. Chan, Y. Kuga, and A. Ishimaru, "Subsurface detection of a target buried in natural media using angular correlation function measurement", *Waves in Random Media*, 7, 457-465, 1997.

Acknowledgement

This research was supported by the National Science Foundation (ECS9522031) and the Office of Naval Research (N00014-97-1-0060).

IX. Figures

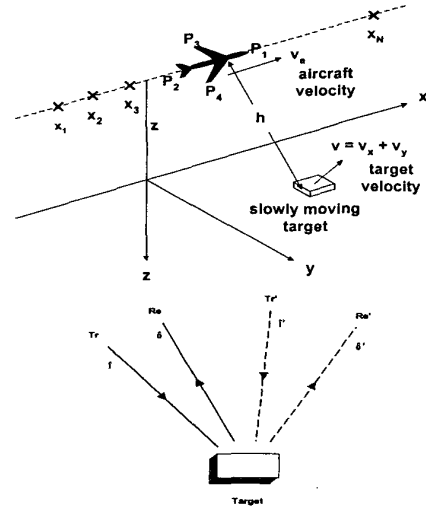


Figure 1: Diagram of the proposed correlation technique. Phases of the correlation functions for the along-track (P_1 - P_2) and across-track (P_3 - P_4) sensors are measured as a function of position x .

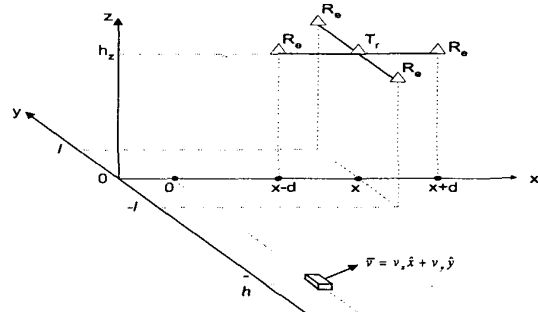


Figure 2: Simulation configuration

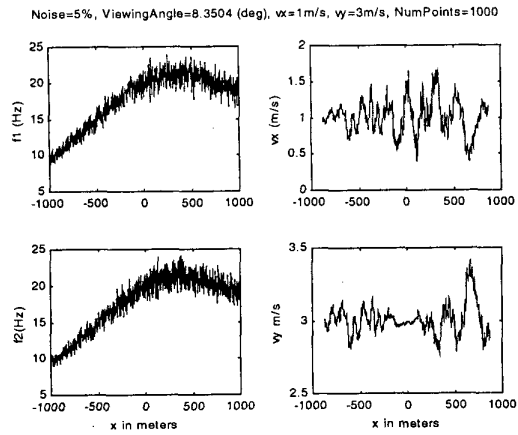


Figure 3: ACT Simulation with Constant Viewing Angle

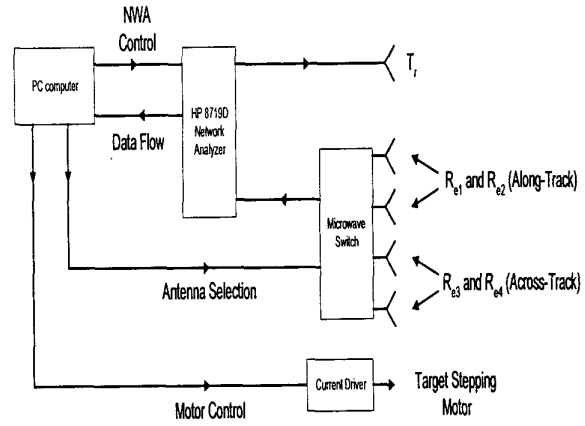


Figure 6: Experimental Control

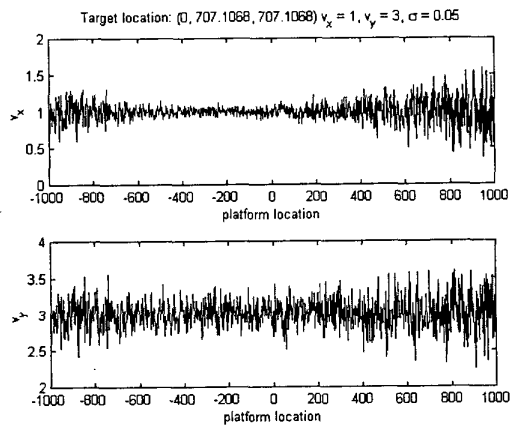


Figure 4: AVT Simulation results, Range = 1km, Angle = 45°

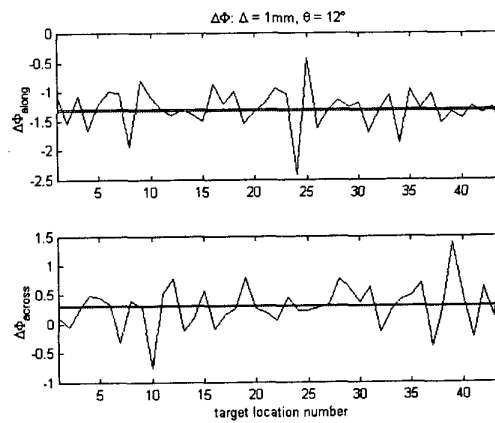


Figure 7: Experimental Results

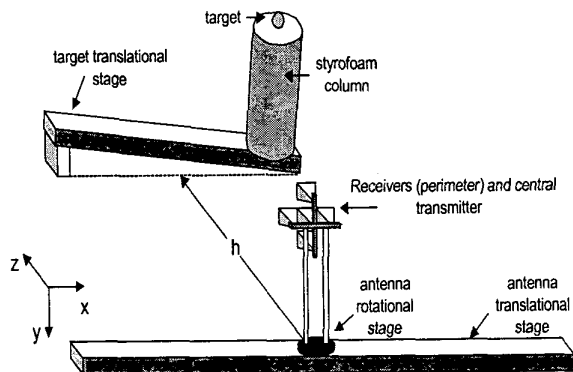


Figure 5: Preliminary Experiment